Advanced Perovskite Materials with Special Properties in Microwave and Terahertz Domains

A. Ioachim, M.I. Toacsan, L. Nedelcu, L. Mihut. A. Szilagyi*

National Institute of Materials Physics, Bucharest-Magurele, RO 077125 ROMANIA
*Military Equipment and Technologies Research Agency, Bragadiru, RO 077025 ROMANIA

SUMMARY

Perovskite $Ba(Zn_{1/3}Ta_{2/3})O_3$ (BZT) ceramics were prepared by solid-state reaction and sintered in air at temperatures in the range 1550-1650 ^oC, for 2 hours. In order to improve the microwave and millimeter wave properties, annealing treatments at 1400 ^oC for 10 hours was applied. The long-range order with a 2:1 ratio of Ta and Zn ions on the octahedral positions of the perovskite structure and the vibrational modes were investigated by using XRD and Raman spectroscopy as function of sintering temperature. Presence of small amount of secondary phase, $Ba_8ZnTa_6O_{24}$, affects Q factor even in the dense, highly ordered samples. The dielectric parameters were measured in the microwave range by Hakki-Coleman method and were correlated with structural and optical properties. Sintering temperature higher than 1600 ^oC are required for BZT ceramics in order to obtain low microwave loss (Q x f ~ 100 THz)

INTRODUCTION

Since 1980's high dielectric constant materials have been developed and put in practical use as resonators for filters in communications, antennas, oscillators, in satellite broadcasting at microwaves and millimeter waves, miniaturizing these components and saving costs. High quality factor (Q) dielectric resonators are required in applications.

Perovskite $Ba(X_{1/3}Ta_{2/3})O_3$ (X=Mg, Zn) ceramics possess a super-high value of the quality factor Q, (> 14,000 at 6GHz) [1] among microwave dielectric materials with low temperature coefficient of resonant frequency (τ_f ~ 5ppm/^{o}C) and a large dielectric constant (ε_r =24-29).

The factors influencing Q values of complex perovskites $Ba(X_{1/3}Ta_{2/3})O_3$ (X=Mg, Zn) have been considered to be long range ordering (LRO) of cations, ZnO evaporation, point defects and stabilization of microdomain boundaries [2]. This explained the high Q values from the point of view of the lattice vibrations of its hexagonal superstructure. Sagala et Nambu [3] calculated the dielectric loss tangent at microwave frequencies from the equation of ion motions which was a function of B-site ordering in the $A(B'_{1/3}B''_{2/3})O_3$ perovskite structure. Galasso and coworkers [4] concluded that the B-site ordering increased as the difference in charge and size between B' and B" atoms increased. The ordering of complex perovskite is important because the 1/3 <111> (1:2) ordering is believed to be closely related to the high-Q property of $Ba(Zn_{1/3}Ta_{2/3})O_3$. There is a strong correlation between the cation ordering, domain growth, zinc or magnesium loss and sintering parameters. Recently, the correlation of B-site ordering with microwave properties in similar ceramics, as elucidated by the Raman method, has been a subject of considerable interest [2, 5–9] A strong relationship between the ordered structure and the remarkable microwave properties has been found. The phonon modes were assigned, and the correlation of phonon vibrations with the microwave properties was found.

In this paper we report the synthesis of $Ba(Zn_{1/3}Ta_{2/3})O_3$ perovskite materials and the correlation between microwave properties, structural parameters and Raman vibrational modes as function on the thermal treatments.

EXPERIMENTAL

$Ba(Zn_{1/3}Ta_{2/3})O_3$ samples were prepared by solid-state reaction [10]. The starting materials were high $BaCO_3$, ZnO and Ta_2O_5 powders. Stoichiometric quantities were weighted, ground, homogenized and milled in an agate mill in water for 5 hours. The powders were calcined at $T = 1200\ ^oC$ for two hours. Then the powders were milled for 3 h and calcined at 1250 ^oC/ 2h. The double calcined powders were mixed with 12 % polyvinyl alcohol (PVA) and dried at $T = 80\ ^oC$, then were pressed into cylindrical samples of 12 mm diameter and 10 mm height. The pellets were slowly dried at 180 ^oC in order to eliminate the PVA.

The density of green ceramics was $\rho = 4.5$ g /cm^3. The sintering treatment for the BZT samples was performed in air for 2 h at three different temperatures: T_s = 1550 ^oC, 1600 ^oC, and 1650 ^oC. In order to improve the dielectric properties, especially the quality factor Q, the samples were treated supplementary for 10 h at 1410 ^oC. The pellets were polished in order to remove the superficial zone and to obtain correct values of the microwave dielectric parameters.

The bulk densities of the sintered pellets were measured by using a water immersion technique. The structure of BZT samples was investigated by X-ray diffraction using a Shimadzu XRD6000 diffractometer with Ni-filtered Cu K_α radiation ($\lambda = 1.5405$ Å). The patterns were recorded at room temperature in a range of 2θ from 15° to 60°.

The Raman studies were performed at room temperature under using a FT Raman spectrometer Bruker RFS 100/S. The 1064 nm output of a YAG-Nd laser was used as the excitation source. Raman spectra have been recorded at 10 mW output power with a resolution of about 1cm^{-1}.

In microwaves, the BZT cylindrical samples exhibit very low dielectric loss, high dielectric constant, and a very good stability with temperature. Therefore, the dielectric parameters of BZT samples were investigated by using the Hakki-Coleman method [11]. A computer-aided measurement system, which combines an HP 8757C network analyzer and an HP 8350B sweep oscillator, was employed for the microwave measurements. The temperature coefficient of the resonant frequency τ_f in the microwave range was measured by heating the samples from +20 ^oC to +80 ^oC.

RESULTS AND DISCUSSION

The bulk densities of the fired BZT ceramics were measured after grinding and polishing. The temperature dependence of the densification after sintering treatment in air for two hours is shown in Fig. 1. The BZT samples treated between 1550 and 1650 ^oC were well sintered. The X-ray density of BZT compound with stoichiometric composition was considered as $\rho = 7.92$ g /cm^3. The best densified ceramic (T_s = 1650 ^oC) exhibits a porosity value of $P \sim 6\%$. The bulk density slightly increases with sintering temperature.

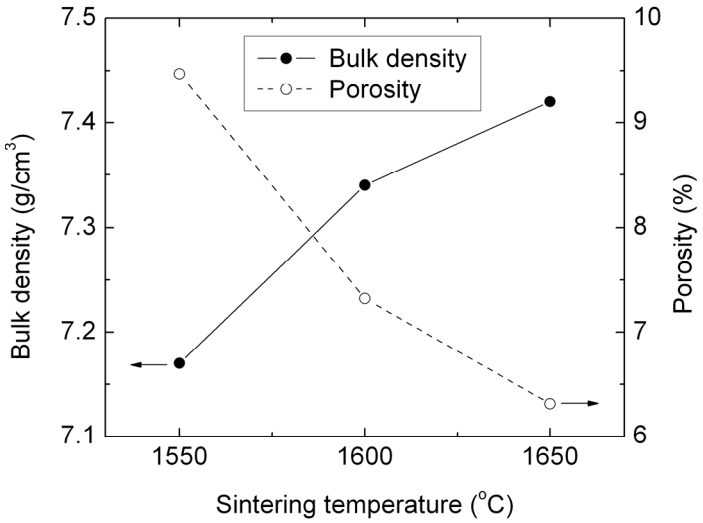

Fig. 1. Bulk density and porosity versus sintering temperature for BZT samples.

The crystal structure of $Ba(Zn_{1/3}Ta_{2/3})O_3$ is of a classic ordered perovskite with two transition metals (B' and B") on the octahedral site. The B' and B" ions occurs on alternating (111) planes in a 1:2 ratio. Each (111) plane contains only one type of small oxygen octahedron, and the planes are ordered in the 1:2 stoichiometric ratio, in the sequence Zn-Ta-Ta-Zn-Ta-Ta- … The resulting symmetry, due to the (111) type plane stacking and accompanying small oxygen displacement strongly depends on processing parameters. Therefore, the ordering of Zn and Ta depends of firing temperature and of the sintering time. The BZT sintered at lower temperatures (T_s < 1300 °C) exhibits a pseudo-cubic perovskite type structure where Zn and Ta are in disorder. At higher sintering temperatures (T_s > 1300 °C) BZT has a hexagonal perovskite type structure, with Zn and Ta showing 1:2 order in the B site. The order of Zn and Ta expands the original perovskite unit cell along the <111> direction and contracts the unit cell in the plane normal to <111>. Consequently, c/a has a value greater than $\sqrt{3/2} \approx 1.2247$ and the unit cell is distorted. The increase of cation ordering on B site in BZT compounds creates a superlattice with a hexagonal structure. The degree of long range-structural order (LRO) can be measured by X-ray methods and it can be expressed as the ratio between the intensity of the super structure reflection and that of a basic unit cell reflection.

Crystallinity and cation ordering of BZT samples were investigated by using powder X-ray diffraction. The mean crystallite size, D, in Å, for these ceramics, can be estimated with the Scherrer equation:

$$D = k\lambda / \beta \cos\theta \qquad (1)$$

where λ is the wavelength, in Å, β is the integrated breadth in radians and θ is the diffraction angle. The instrument contribution to the FWHM for the (100), (102) and (110) reflections is 0.157° 2θ and k was established at the value 0.9. The calculated crystallite sizes as well as the unit cell parameters are presented as function of sintering temperature in Table 1. The degree of cation ordering based on the supercell (100) and subcell ((110)+(102)) peaks are summarized in Table 1, too. In this case the normalized intensity ratio, IR, defined as

$$IR = I(100) / [I((110) + (102)) \times 0.032] \qquad (2)$$

where I denotes the integrated intensities of the subcell and supercell reflections and 0.032:1 is the expected integrated integrated intensity ratio of these reflections for a fully ordered phase. This permits the deduction of the long-range order (LRO) parameter, S , from the equation (2)

$$S = \sqrt{IR} \tag{3}$$

The X-ray diffraction patterns for BZT compound, sintered at 3 temperature values are given in Fig. 2. The patterns confirm the formation of the hexagonal structure, which is the majority phase. For the BZT compounds sintered at T_s =1600 °C and 1650 °C the XRD patterns reveal the presence of secondary phase $Ba_8ZnTa_6O_{24}$, which disappear at lower sintering temperatures.

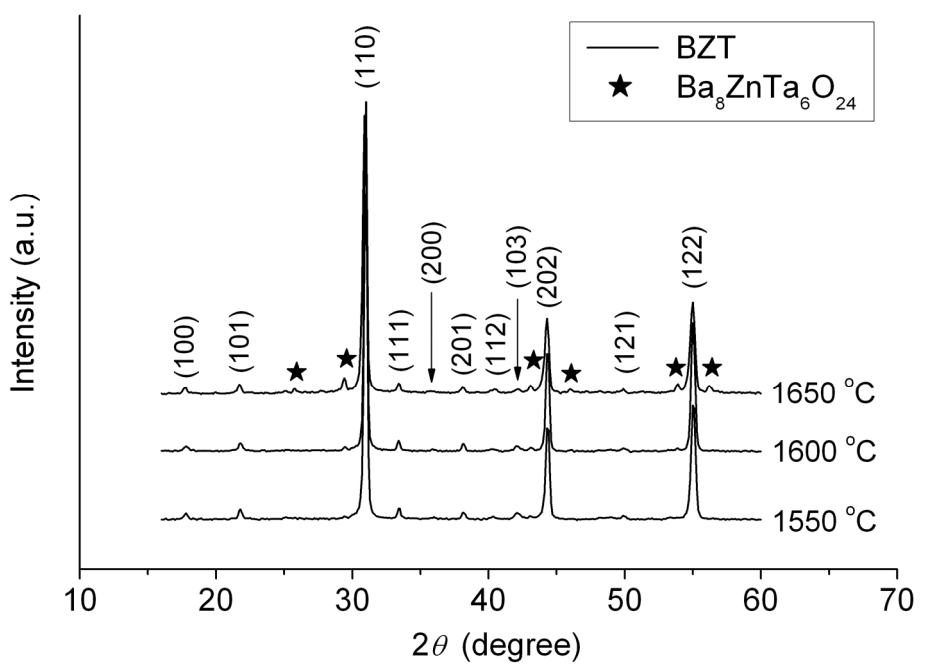

Fig. 2 X-ray diffraction patterns of BZT samples versus sintering temperature

The structure order was evidenced from the XRD patterns by observing the reflections due to Zn and Ta order (superstructure reflection) and the line split, i.e the c/a differs of $\sqrt{3/2}$. The former shows the amount of Zn and Ta ordering and the latter shows the lattice distortion by Zn and Ta ordering. In the superstructure lines, the reflections whose index (2h + k + l) / 3 does not equal the integer, are caused by the Zn and Ta. Therefore, a change in intensity of the superstructure reflection corresponds to the amount of Zn and Ta order. The (100) reflection has the strongest intensity among the superstructures lines. Fig.2 shows the increase in intensity of (100) reflection versus sintering temperature for 2h. LRO gradually increase up to 1650 °C. Table 1 presents the main structural parameters as a function of sintering temperature.

Table 1. Structural parameters of BZT samples versus sintering temperature.

Sample	Sintering temperature (°C)	Unit cell parameters				Mean crystallite size D (Å)	LRO parameter S
		a_o (Å)	c_o (Å)	c_o/a_o	V_o (Å^3)		
1	1550	5.774	7.093	1.2252	205.84	676	0.79
2	1600	5.785	7.091	1.2257	205.36	687	0.81
3	1650	5.773	7.089	1.2279	204.60	744	0.86

The perfectly ordered structure is produced by the following process:

1. A perovskite-type structure is formed, but Zn and Ta are in disorder
2. Zn and Ta are partially in order
3. Zn and Ta are completely in order and the lattice is distorted.

A supplementary distortion can be produced by the ZnO loss. At high sintering temperatures, ZnO evaporates. The Zn^{2+} ions on B'- site are partially replaced by Ba^{2+}, which have a much larger ionic size 1.61 Å comparatively to 0.74 Å for Zn. This substitution creates a supplementary unit cell distortion, even when the LRO is saturated and leads to an increase of Q. The ZnO loss is evidenced in Fig. 3, where the X-ray diffraction patterns indicate the appearance of $Ba_8ZnTa_6O_{24}$ secondary phase, especially at surface of the sample.

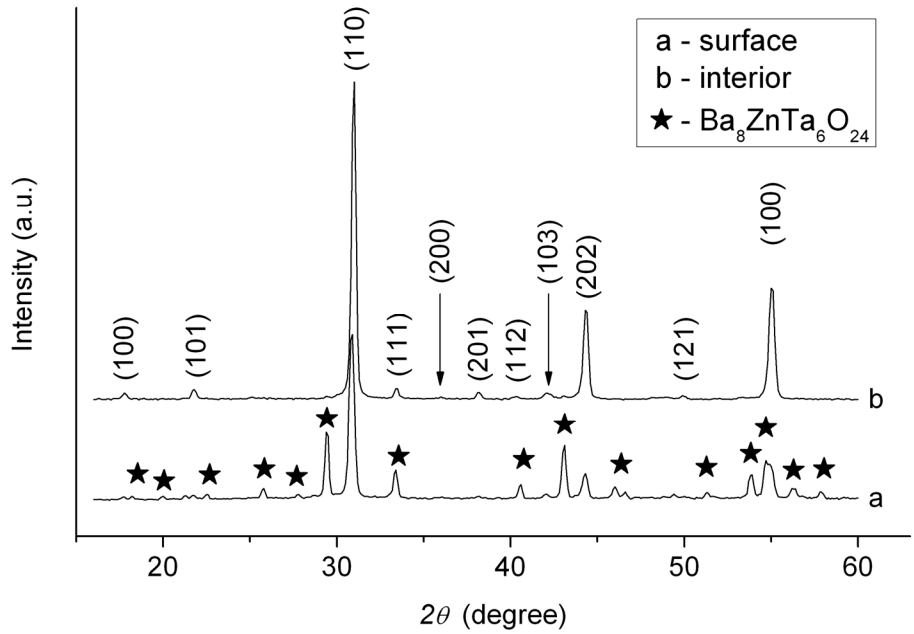

Fig. 3. X-ray diffraction patterns of BZT sample sintered at 1650 °/2h with annealing at 1410 °C/10h

Raman scattering is highly sensitive method to determine the composition of materials. Therefore, the Raman spectroscopy provides important information that correlates the vibration characteristics of the materials with the microwave dielectric properties, even though the Raman phonons of the complex perovskite materials which are mainly nonpolar.

The variations of shift and full width at half maximum (FWHM) Raman lines for BZT are two important fingerprints in identifying the normal modes.

From the viewpoint of the lattice vibration, a BZT crystal with an ideal cubic perovskite structure (space group of *Pm3m* symmetry, in which the B-site cations are randomly distributed) does not show any Raman active mode. However, a 1:1 ordered perovskite with a space group of *Fm3m* symmetry allows for four strong Raman lines [8]:

$$\Gamma = A_1g[O] + E_2g[O] + 2F_2g[A + O], \quad (4)$$

where the square brackets shows the ions involved in a particular normal vibration mode. On the other hand, the 1:2 ordered perovskite structure based on P3m1 symmetry gives nine Raman active modes [5]:

$$\Gamma = 4A_1g[A,B'', O] + 5Eg[A,B'', O] \quad (5)$$

The typical Raman spectra of BZT have four main peaks, as discussed in Ref. 5; they are assigned to normal vibration modes related to the localized 1:1 ordered structure, [5, 6] although the long-range 1:2 order is preserved. The Raman spectra of the normal vibrations of localized 1:1 ordered and long-range 1:2 ordered structure consist of four key features: 1) the Raman phonon with the lowest energy near 104 cm^{-1} corresponds to $F_2g(Ba)$ of the 1:1 ordered structure; 2) two modes associated with the vibration of O atoms at 375 cm^{-1} and 424 cm^{-1} ($F_2g(O)$ and $Eg(O)$); 3) the broad peak near 807 cm^{-1}, which corresponds to $A_1g(O)$ of the 1:1 ordered structure is the stretch mode of the oxygen octahedron; 4) three more weak phonons are also detected between 150 and 300 cm^{-1}, and they are strongly related to the long-range 1:2 ordered structure. According to these 4 features, the obtained Raman spectra for BZT calcined at 1250 ^{o}C/2h and the sample sintered at 1550 ^{o}C/2h are depicted in Fig. 4. It was expected that the calcined powder would have a cubic perovskite structure and thus show no Raman lines. However, are no significant differences in shape intensities and position between calcined and sintered sample for Raman lines corresponding to 1:1 ordering. The 1:2 ordering is not well evidenced for calcined samples. The 3 extralines in three range of 150 - 300 cm^{-1} are the characteristic feature of the 1:2 ordered perovskite and these can be observed for the sintered sample.

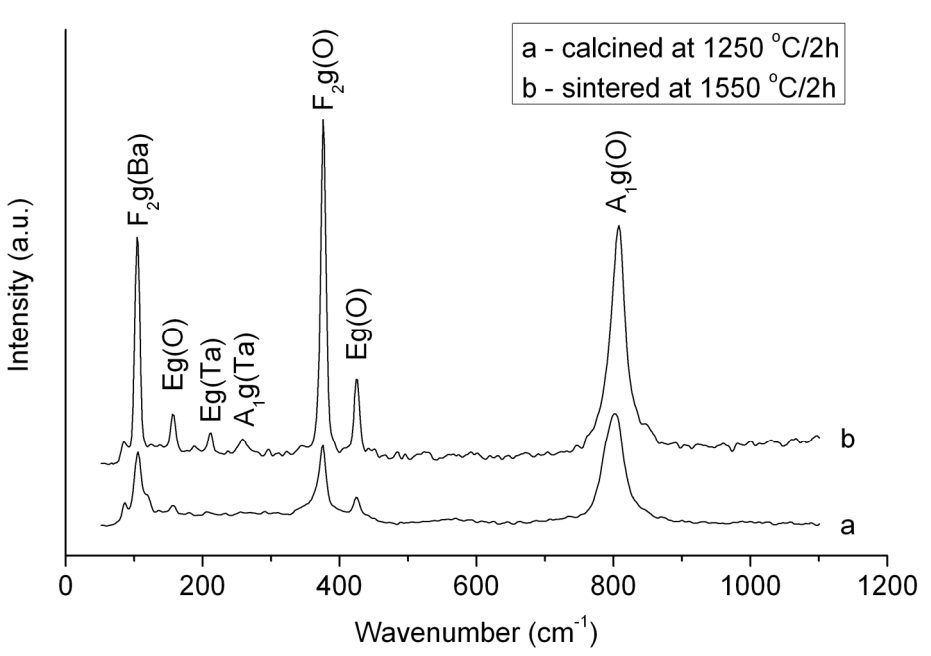

Fig. 4. Raman spectra for BZT sample calcined at 1250 °C and sintered at 1550 °C/2h

The ZnO evaporation during thermal treatments at the samples surface was evidenced also by Raman spectroscopy. Fig. 5 shows the Raman spectra for the interior and surface of the BZT samples sample sintered at 1650 °/2h with annealing at 1410 °C/10h. The surface Raman spectrum presents two supplementary peaks shifted to lower wavenumber, one near 780 cm^{-1} and the other near 360 cm^{-1}, corresponding to the $Ba_8ZnTa_6O_{24}$ secondary phase.

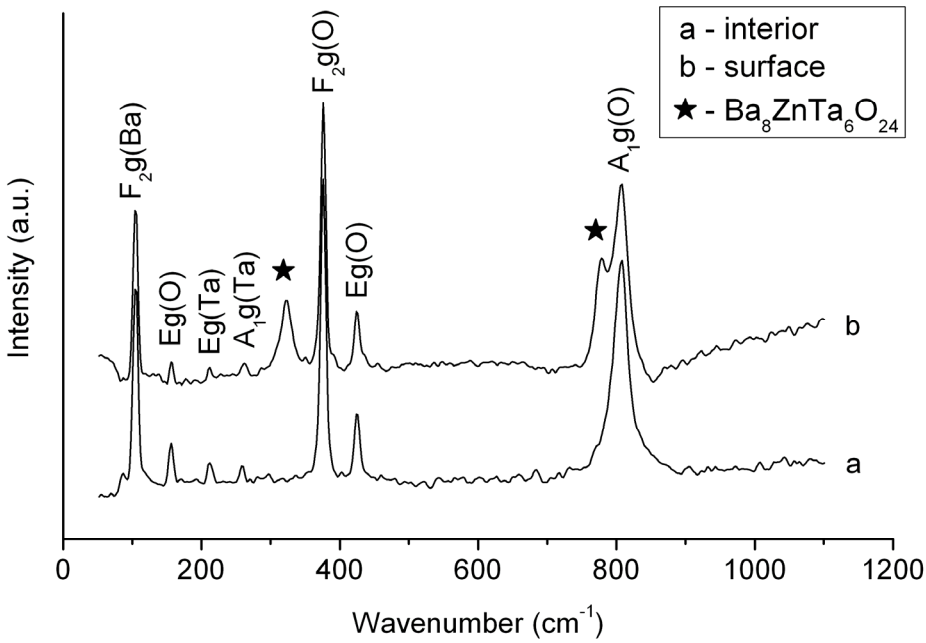

Fig. 5. Raman spectra of BZT sample sintered at 1650 °/2h with annealing at 1410 °C/10h

Microwave measurements on dielectric constant and loss tangent were carried out on the BZT dielectric resonators. The obtained data revealed a determinant influence of the sintering temperature on the complex dielectric constant. The variation of the dielectric constant and quality factor with the sintering temperature can be observed from Table 2. This can be considered as an effect of the reduced porosity resulting in a better densification at high sintering temperatures, as can be seen in Fig. 1.

Table 2. Microwave dielectric parameters of BZT sintered resonators versus sintering temperature.

Sample	Sintering temperature T_s (°C)	Resonance frequency f (GHz)	Dielectric constant ε_r	Dielectric loss $tan\ \delta$ (x 10^{-4})	Quality factor Q	τ_f (ppm/°C)
1	1550	5.84	25.7	1.28	7800	+3 ÷ +6
2	1600	5.74	26.9	1.01	9900	
3	1650	5.67	27.9	0.81	12400	

The additional thermal treatment at 1410 °C for 10 h for all BZT samples resulted in the increase of the dielectric constant and of the quality factor as can be seen in Table 3. The dielectric constant values were not substantially modified by the annealing treatment. On the other hand, for annealed samples, the quality factor substantially increases for samples sintered at 1650 °C/2h.

The BZT dielectric resonators exhibit a positive temperature coefficient of the resonance frequency τ_f in the 3 ÷ 6 ppm/ °C range.

Table 3. Microwave dielectric parameters of BZT resonators annealed at 1410 °C/ 10h versus sintering temperature

Sample	Sintering temperature T_s (°C)	Resonance frequency f (GHz)	Dielectric constant ε_r	Dielectric loss $tan\ \delta$ (x 10^{-4})	Quality factor Q	τ_f (ppm/°C)
1	1550	5.82	26	1.06	9400	+3 ÷ +6
2	1600	5.73	27.1	0.95	10500	
3	1650	5.67	28	0.56	17600	

For dielectric resonators, in the microwave and millimeter wave domain, the product between the resonance frequency f and quality factor Q is constant [12]. Consequently, the product Q x f is more frequently encountered as resonator parameter rather than the quality factor. The influence of the annealing treatment on dielectric constant and the Q x f product of BZT resonators is presented in Fig. 6. The Q x f value increases especially for samples sintered at 1650 °C/2h and takes values up to 100 THz. On the other hand, the annealing treatment slightly increases the dielectric constant.

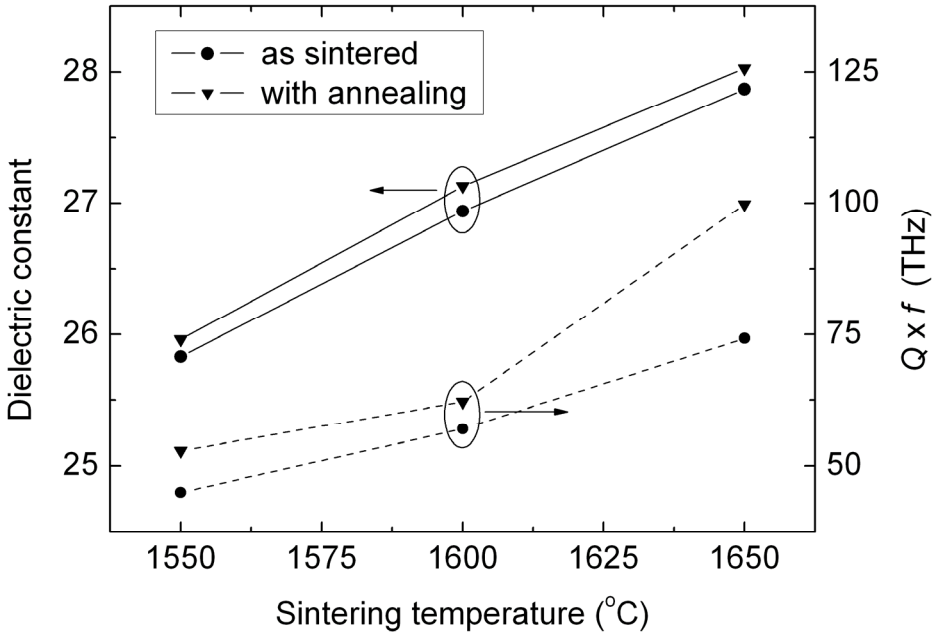

Fig.6 Dielectric constant and *Q* x *f* product versus sintering temperature for BZT sintered and annealed resonators.

In order to evaluate the relationship between the ordering, the normal vibration modes and *Q* x *f* product the LRO parameters *S*, the FWHM of the $A_1g(O)$ Raman line were investigated. The calculated data for annealed BZT samples as function of the sintering temperature are presented in Table 4.

Tab. 4. *Q* x *f* product, FWHM of the $A_1g(O)$ Raman line and LRO parameters *S* for annealed BZT samples versus sintering temperature

Sample	Sintering temperature (°C)	*Q* x *f* Product (THz)	FWHM $A_1g(O)$ (cm^{-1})	LRO parameter *S*
1	1550	52.8	25.47	0.79
2	1600	62.2	24.75	0.81
3	1650	99.8	24.43	0.86

There are not shift observed for $A_1g(O)$ Raman lines, only the intensity slowly decreases with the increasing of the sintering temperature. The same behavior presents the 3 Raman lines Eg(O), Eg(Ta) and $A_1g(Ta)$ corresponding to the 1:2 ordered structure. In the same time, the FWHM for $A_1g(O)$ Raman line decreases with the increasing of the sintering temperature.

From XRD and Raman analysis it was concluded that the increase of sintering temperature and annealing treatments improves the cation ordering in BZT ceramics, which leads to higher values of *Q* x *f* product. Moreover, the XRD and Raman investigation evidenced the appearance of the Zn-poor secondary phase at the BZT sample surface. *Q* x *f* product values monotonically increases with the LRO parameter increase and with the decrease of the FWHM for $A_1g(O)$ Raman line.

The high values of $Q \times f$ product obtained for BZT resonators sintered at 1650 °C/2h and annealed at 1410 °C/10h recommend this type of materials for applications in component manufacturing for millimeter and sub-millimeter wave domain.

CONCLUSIONS

$Ba(Zn_{1/3}Ta_{2/3})O_3$ dielectric materials with high dielectric constant and low loss in microwave domain were achieved by solid-state reaction and sintered in the temperature range 1550 ÷ 1650 °C for 2h. It was shown that the additional annealing treatment at 1410 °C for 10 hours improves the microwave dielectric parameters.

The X-ray diffraction patterns confirm the formation of the BZT materials with hexagonal structure. For sintering temperatures higher than 1600 °C, the XRD patterns reveal the BZT multiphase compositions with a secondary phase with low Zn content.

The dielectric constant and $Q \times f$ product increase with the increasing of the sintering temperature. The annealing has small effect on the dielectric constant value. On the other hand, the $Q \times f$ product substantially increases after annealing, especially for samples sintered at 1650 °C/2h. The temperature coefficient of the resonance frequency exhibits positive values less than 6 ppm/ °C.

The high-Q BZT materials possess sharpest vibrational modes, that mean smallest FWHM value for Raman peaks. The intimate relationship between the phonon characteristics and the fine structure of the materials is confirmed.

Well-sintered and annealed BZT resonators exhibit a dielectric constant around 28, τ_f in the 3 ÷ 6 ppm/ °C range and a $Q \times f$ product up to 100 THz. The achieved high values of the quality factor Q as well as the very low variation with the temperature of dielectric constant recommend the BZT materials for mm-wave and terahertz domain applications.

ACKNOWLEDGMENTS

This work was supported by Ministry of Education and Research under contract CEEX no. 4/2005.

BIBLIOGRAFIE

[1] T. Shimada, "Far-infrared reflection and microwave properties of $Ba([Mg_{1-x}Zn_x]_{1/3},Ta_{2/3})O_3$ ceramics", J. Eur. Ceram. Soc. 24, 2004, pp. 1799-1803

[2] H. Tamura et all, "Lattice Vibrations of $Ba(Zn_{1/3}Ta_{2/3})O_3$ Crystal with Ordered Perovskite Structure", Jpn. J. Apl. Phys. 25(6), 1986, pp. 787-91

[3] D.A. Sagala, S. Nambu, "Microscopic calculation of Dielectric Loss at Microwave Frequencies for Complex Perovskite $Ba(Zn_{1/3}Ta_{2/3})O_3$", J.Am. Ceram.Soc. 75(9), 1992, pp. 2573-2575

[4] F. Gallasso, J. Pyle, "Ordering in Compounds of the $A(B'_{1/3}Ta_{2/3})O_3$ Type", Inorg. Chem. 2 (3), 1983, pp. 482-484

[5] I.G. Siny, R.W. Tao, R.S. Katiyar, R.A. Guo, A.S. Bhalla, "Raman spectroscopy of Mg–Ta order–disorder in $BaMg_{1/3}Ta_{2/3}O_3$", J. Phys. Chem. Solids., 1998, 59, 181–195.

[6] S.J. Webb, J. Breeze, R.I. Scott, D.S. Cannell, D.M. Iddles, N.McN. Alford, "Raman Spectrocopic Study of Galium-Doped $Ba(Zn_{1/3}Ta_{2/3})O_3$", J. Amer. Ceram. Soc. 85, 2002, pp. 1753-1756

[7] C.-T. Chia, Y.-C. Chen, H.-F. Cheng, I.-N. Lin, "Correlation of microwave dielectric properties and normal vibration modes of $xBa(Mg_{1/3}Ta_{2/3})O_3$–$(1-x)Ba(Mg_{1/3}Nb_{2/3})O_3$ ceramics: I. Raman spectroscopy", J. Appl. Phys., 2003, 94, 3360–3364.

[8] C.J. Lee, G. Pezzotti, Shin H. Kangb, Deug J. Kimb, Kug Sun Hong, "Quantitative analysis of lattice distortion in $Ba(Zn_{1/3}Ta_{2/3})O_3$ microwave dielectric ceramics with added B_2O_3 using Raman spectroscopy",

[9] J. Eur. Ceram. Soc. 26 (2006) 1385–1391

[10] H.-F. Cheng, C.-T. Chia, H.-L. Liu, M.-Y. Chen, Y.-T. Tzeng, I.-N. Lin, "Correlation of the phonon characteristics and microwave dielectric properties of the Ba(Mg1/3Ta2/3)O3 materials", J. Eur. Ceram. Soc. 27 (2007) 2893-2897

[11] A. Ioachim, L. Nedelcu, E. Andronescu, S. Jinga, M. I. Toacsan, M. G. Banciu, A. Lörinczi, M. Popescu, "The effects of thermal treatments on microwave dielectric properties of $Ba(Zn_{1/3}Ta_{2/3})O_3$ ceramics", J. Optolectron. Adv. Mater. 10, 2008, pp. 209-212

[12] B.W. Hakki, P.D. Coleman, "A dielectric resonator method of measuring inductive capacities in millimeter range", IRE Trans. Microwave Theory Tech., 1960, MTT 8, pp. 402-410

[13] Y. Higuchi, H. Tamura, Recent progress on the dielectric properties of dielectric resonator materials with their applications from microwave to optical frequencies, Journal of the European Ceramic Society, Vol. 23, 2003, pp. 2683–2688